Extension of the ECRH Operational Space with O2- and X3-Heating Schemes to control Tungsten Accumulation in ASDEX Upgrade

H. Höhnle 1), J. Stober 2), A. Herrmann 2), W. Kasparek 1), F. Leuterer 2), F. Monaco 2), R. Neu 2), D. Schmid-Lorch 2), H. Schütz 2), J. Schweinzer 2), U. Stroth 1), D. Wagner 2), S. Vorbrugg 2), E. Wolfrum 2) and the ASDEX Upgrade Team

1) Institut für Plasmaforschung, Universität Stuttgart, Stuttgart, Germany
2) Max-Planck-Institut für Plasmaphysik, EURATOM-Association, Garching, Germany

E-mail contact of the main author: hoehnle@ipf.uni-stuttgart.de

Abstract. ASDEX Upgrade is operated since several years with tungsten coated plasma facing components. H-mode operation with good confinement has been demonstrated. Nevertheless purely NBI-heated H-modes with reduced gas puff, moderate heating power or/and increased triangularity tend to accumulate tungsten, followed by a radiative collapse. Under these conditions, central electron heating with ECRH (X2) changes the impurity transport in the plasma center, reducing the central tungsten concentration and, in many cases, stabilizing the plasma. In order to extend the applicability of central ECRH to a wider range of magnetic field and plasma current additional ECRH schemes with reduced single pass absorption have been implemented: X3 heating allows to reduce the magnetic field by 30 %, such that the first H-modes with an ITER-like value of the safety factor $q_{95} = 3$ could be run in the tungsten-coated device. O2 heating increases the cutoff density by a factor of 2 allowing to address higher currents and triangularities. In case of central X3 heating, the X2 resonance lies close to the pedestal top at the high-field side of the plasma, serving as a beam dump. For O2, holographic mirrors have been developed which guarantee a second pass through the plasma center. The beam position on these reflectors is controlled by fast thermocouples. Stray-radiation protection has been implemented using sniffer-probes.

1. Introduction

The ECRH system at ASDEX Upgrade consists of four "old" gyrotrons at 140 GHz, each delivering a power of 0.5 MW over 2 s, and a new system, which is currently installed. The new ECRH system will consist of four multi-frequency gyrotrons delivering 1 MW over a complete ASDEX Upgrade discharge (10 s). The typically used second harmonic extraordinary mode (X2 mode) at 2.5 T has the advantage of a complete and localized absorption. These two systems were especially designed for transport studies with local electron heating and MHD control with ECCD. A new application was found when the first wall material at ASDEX Upgrade was changed from carbon to the high Z material tungsten. In improved H-modes with low gas puff the plasma tends to accumulate tungsten, followed by a radiation collapse. In such discharges central ECRH leads to a modification of the tungsten transport and to a reduction of the tungsten concentration in the plasma center [1,2,3].

However, the usage of central X2 heating with 140 GHz in the plasma center requires $B_t \approx 2.5$ T and $n_e(0) < 1.2 \cdot 10^{20}$ m^{-3} (X2 cutoff). The latter is in conflict with the requirement of ITER-like discharges to be operated at a safety factor of $q_{95} \approx 3$ at $70 - 90$ % of the density limit $n_{GW} > 1.7 \cdot 10^{20}$ m^{-3}. The X2 cutoff limits H-mode operation close to this density limit with central heating to $q_{95} > 4.5$ depending on plasma shape. To protect in vessel components from ECRH stray radiation when operating the ECRH close to the cutoff, sniffer probes [4] were installed at ASDEX Upgrade, measuring the reflected microwave power. With these probes a real time interlock is realized to switch off the ECRH while reaching a cutoff. Here two schemes are presented which circumvent the limitation of ECRH for ITER-like H-mode operation.

One ansatz to avoid cutoffs at $q_{95} \approx 3$ is to reduce the magnetic field by 30 %, where the third harmonic extraordinary mode (X3 mode) is absorbed in the core. However this mode suffers from incomplete absorption [5] at usual electron temperatures of 3 – 5 keV. This heating scenario is described in section 2.1 and the experimental results are presented in section 4.1.

An alternative is to use the ordinary mode (O2 mode) at the second harmonic of the resonance at $B_t = 2.5$ T. This mode has a cutoff at the plasma frequency, which is equivalent to twice the cutoff density of the X2-mode cutoff. But the disadvantage of the O2 mode is also an incomplete absorption [5] at typical electron temperatures of 3 – 4 keV. To increase the optical thickness $\tau \sim T_e^2$ [6], a mirror for a second pass of the beam through the plasma is mounted at the inner column of ASDEX Upgrade. The design of the mirror and the associated heating scenario are described in section 3 and 2.2, respectively. First experimental results with a second pass of the beam are shown in section 4.2 and 4.3. Finally, the paper is summarized and the results are discussed in section 5.

2. Heating Scenarios

To develop new ECRH scenarios in high density plasmas or at lower magnetic fields the beam tracing code TORBEAM [7] was used, which calculates the trace, the deposition and the current drive profiles of the ordinary and extraordinary beam for different injection angles, magnetic configurations, density and temperature profiles.

2.1 X3-Heating Scenario

For the X3-heating scenario a central deposition of the ECR power is realized at a toroidal field of $B_t \approx 1.7$ T. At this field a q_{95} of about 3 is achieved at a plasma current of 1 MA. But for the accessible plasma parameters in ASDEX Upgrade the absorption is incomplete. To handle the shine-through power the magnetic field is increased to 1.8 T; thereby the resonances are shifted to the low field side such that the X2 resonance is shifted from the SOL on the high field side to the pedestal top (Fig. 1), where the shine-through is completely absorbed [8]. In this scenario the X3 resonance is shifted by a few cm from the axis, but the absorption of the X3 resonance is still central enough to avoid tungsten accumulation. The TORBEAM simulation (Fig. 1) shows a central absorption of $\approx$ 70 % at $\rho < 0.2$ (see also [9]) for realistic plasma parameters of $n_e(0) = 1.0 \cdot 10^{20}$ m^{-3} and $T_e(0) = 2.5$ keV.
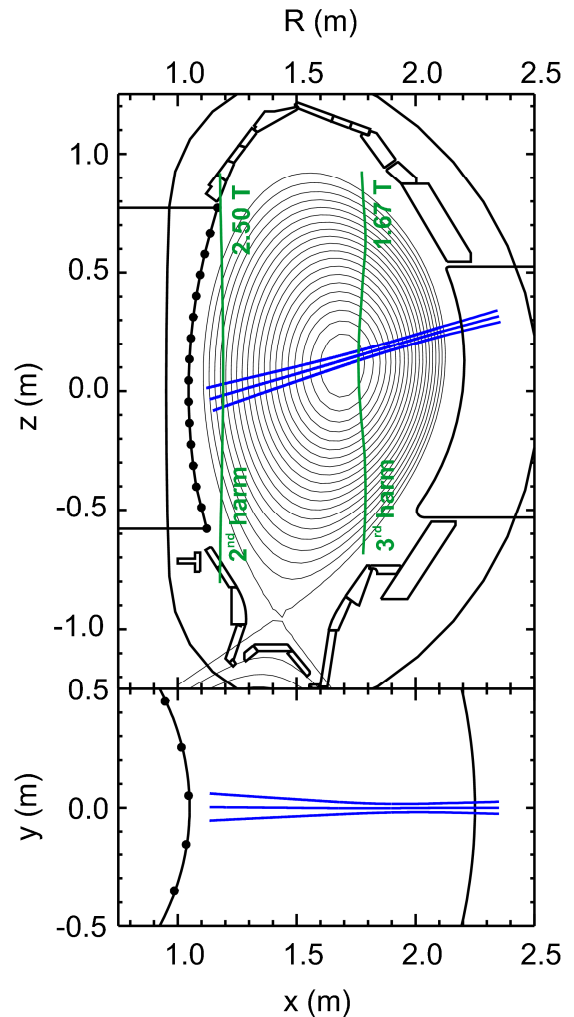

FIG. 1: *Poloidal and toroidal cross section of ASDEX Upgrade with resonant layers and injection paths calculated by TORBEAM for the X3-heating scenario.*
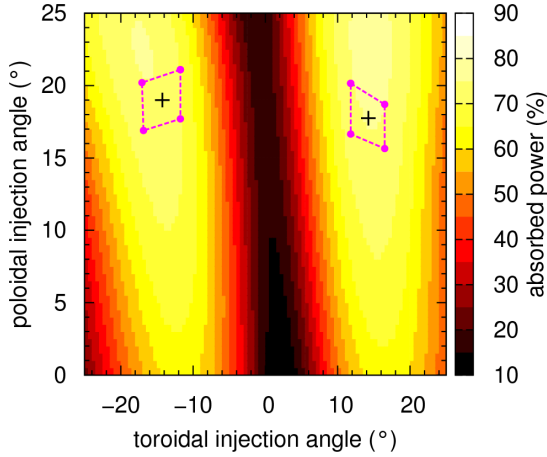
2.2 O2-Heating Scenario

FIG. 2: Absorption of O2-mode heating at ASDEX Upgrade with $n_e(0) = 1.4 \cdot 10^{20}$ m^{-3}, $T_e(0) = 3.5$ keV obtained from TORBEAM calculations for different toroidal and poloidal injection angles. The crosses show the central hit of the beam with the holographic mirrors (dimensions in violet lines).

To investigate the O2-heating scenario with the TORBEAM code, expected plasma parameters for a 1.4 MA discharge were chosen ($n_e(0) = 1.4 \cdot 10^{20}$ m^{-3}, $T_e(0) = 3.5$ keV). For these parameters the theory predicts an optical thickness of approximately 2 (absorption up to 86 %) for an optimal injection angle of $\approx 15°$ [5,6,10].

The TORBEAM calculations were done for different poloidal (θ) and toroidal (φ) injection angles for the new steerable launcher [11]. The absorbed power for the different angles is plotted in Fig. 2 as a contour plot. The bright and dark colours are linked to regions with high and low absorption, respectively. As expected, the highest absorptions of ≈ 80 % can be achieved at around $\varphi = 15°$. Because of this incomplete absorption, the machine safety is not guaranteed and problems with localised stray radiation are expected. Therefore, the non-absorbed power must be further reduced. The only possibility to raise the absorption of the ECRH beam in O2 mode is a second pass of the beam through the plasma. Mirrors installed at the inner column of ASDEX Upgrade can handle this problem; the design of such mirrors is described in more detail in section 3.

The poloidal and toroidal cross section of the configuration used is shown in Fig. 3. The blue curve illustrates the first and the red the second pass of the beam through the plasma. The violet region at the inner wall of ASDEX Upgrade shows the location of the holographic mirrors. The chosen injection angles were optimized for good absorption **and** central hit on the mirrors, therefore they differ slightly from the optimal injection angle. Nevertheless, the absorption can be
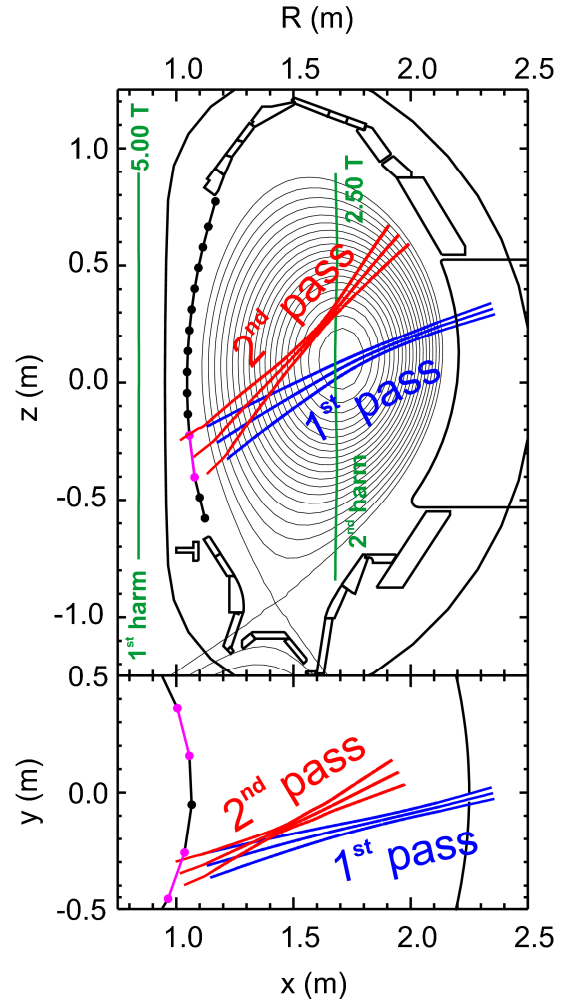

FIG. 3: Similar to Fig. 1 but for the O2-mode heating scenario with the beam launched from the new steerable launcher.

increased up to 94 %, instead of 75 % at single pass. The injection angles with the central hit of the beam on the mirrors are marked as crosses in Fig. 2, also the dimensions of the mirrors are shown as violet lines. The second reflection is on the passive stabilisation loop, where no sensitive components are mounted. The stray radiation will be further reduced when passing a third time through the plasma, but this has not been analysed numerically.

3. Design of the Mirrors

As described in section 2.2, a second pass of the O2-mode beam should be realized by mirrors at the inner wall of ASDEX Upgrade. These reflectors must fulfil some conditions which are essential for the safe operation of such a reflector in ASDEX Upgrade:

1. The mirrors must be conformal to the inner wall, to not suffer from erosion and disturb or pollute the plasma
2. The mirrors have to be polarization independent, which means that the incoming O-mode beam is also reflected as beam in ordinary polarization
3. The reflection must be directed and refocused to the plasma core to achieve an optimal second absorption ($\approx 15°$ toroidal injection)

These terms are only complied for holographic or phase grating mirrors. To design such gratings, the phase front as well as the incoming and outgoing angles of the beams on the surface of the mirrors have to be known. This can be extracted from the TORBEAM simulations. To ease the manufacturing and the later operation some more conditions must be fulfilled:

4. The curvature of the grating profile has to be smooth in order to avoid high electric fields on the mirror surface and erosion of sharp structures
5. The milling tool limits the maximal slope angles of the grating profiles

In order to design high efficiency mirrors under these constraints, an optimization code, based on a differential evolution algorithm [12], was developed. The optimization process corresponds to a minimization of a cost function C, which includes all the above mentioned conditions:

$$C = (1 - \eta_{circ}) + \varepsilon_{curv} + \varepsilon_{angle}$$

Where η_{circ} is the efficiency of the grating for circular polarization, taking into account the efficiency in TE and TM polarizations as well as the phase shift between these two polarizations. This efficiency is computed with a boundary element code [10]. The other two terms are geometrical factors. ε_{curv} is the curvature term, which is small for a flat profile and high for a sharply peaked profile. The ε_{angle} includes the condition of the limitation of the milling tool. During the optimization process it was found that the third order of diffraction of a grating implements all these condition at best. Hence this order was chosen for the mirror. Under all these issues mirrors with ≈ 90 % efficiency could be calculated and manufactured. Resonator measurements of the reflectivity of the mirrors show good agreement with the expected values.

Another issue is to keep the high power beams focused on the mirrors. A new beam position detection system, based on ohmic losses of the microwave on the mirror surface, was installed. With thin NiCr-Ni thermocouples (diameter 0.25 mm and only a few ms rise time) it is foreseen to react on beam movements, caused for example by density changes, in real time by adjusting the poloidal injection angle with the fast steerable launcher [11]. The toroidal injection angle cannot be changed during the discharge, but TORBEAM calculations have shown, that this angle does not change that much during density changes and therefore can be fixed before the discharge.

4.   Experimental results

4.1 Experiments with X3-mode heating

Fig. 4 shows the successful suppression of tungsten accumulation using X3 heating with an X2 beam dump at the plasma edge. Control parameters in both discharges differ only by the amount of ECRH power. In the discharge on the left the ECRH power of 1 MW was not sufficient to suppress the tungsten accumulation. The tungsten concentration rises and the electron temperature decreases due to higher radiation losses. At 2.7 s the temperature is reduced dramatically, such that the X2 resonance in the pedestal top cannot act as beam dump anymore, which induces a rise of the sniffer signal. In contrast to this behaviour, the doubled ECRH power in #25797 prevents the increase of the tungsten concentration in the core and stabilizes the plasma.
A discharge at q_{95} = 3 was also successfully carried out as discussed in Ref. [9].
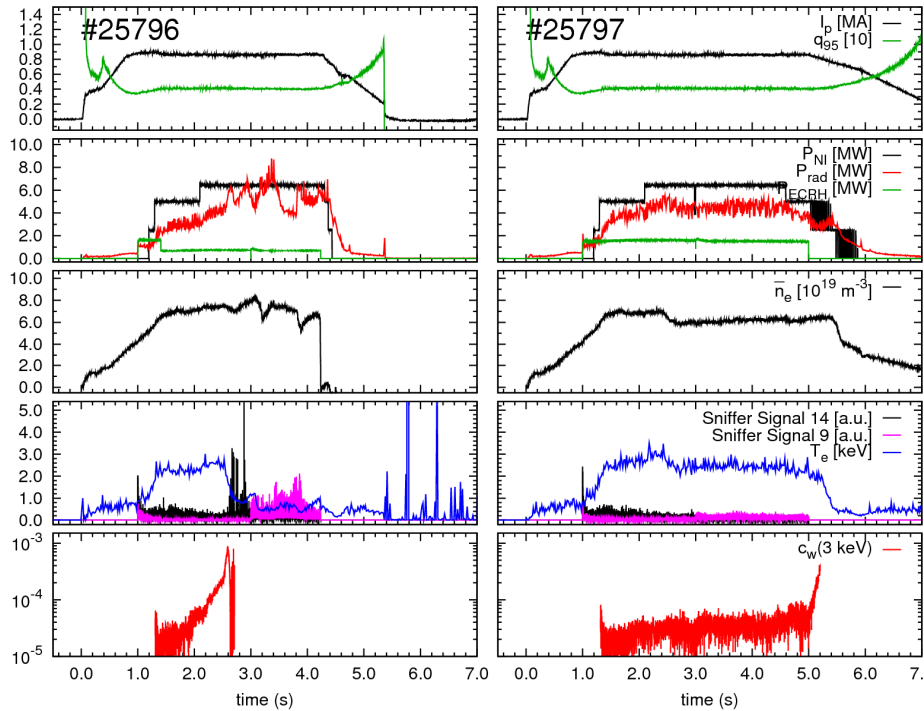

FIG. 4: Identical X3 mode heated discharges differing only in the injected ECRH power. The stray radiation rises during the decrease of the temperature caused by radiation cooling of the tungsten accumulation.

4.2 Test of the O2 reflector

The new reflector tiles had to be tested with respect to the suitability of the embedded thermocouples and with respect to its capabilities in reflecting the non-absorbed power towards the plasma center. The thermocouples were tested with high power microwaves of 0.4 MW for 100 ms injected into the empty vacuum vessel of ASDEX Upgrade. In a scan over the whole surface of one mirror by changing the angles of the microwave launcher the behaviour of the thermocouples could be demonstrated. It was found that the thermocouples show a clear rise of their temperature ($\Delta T \approx 30$ °C) only if the beam hits their direct neighbourhood (a few cm) within

a few 10 ms. Thus it is possible to use their signals for the localization of the microwave beam on the holographic mirrors. The thermocouple signals of a discharge with plasma are shown in Fig. 5. The O2-mode beam (switched on in the grey region) was moved from above the mirror to the center and back (launcher mirror movement is marked as violet line). The red (a) and green (b) curves belong to the thermocouples marked with crosses in the same colour. The higher gradient in the temperature of the upper thermocouple during the movement of the beam seems suitable for a feedback control of the launcher angle in the future.
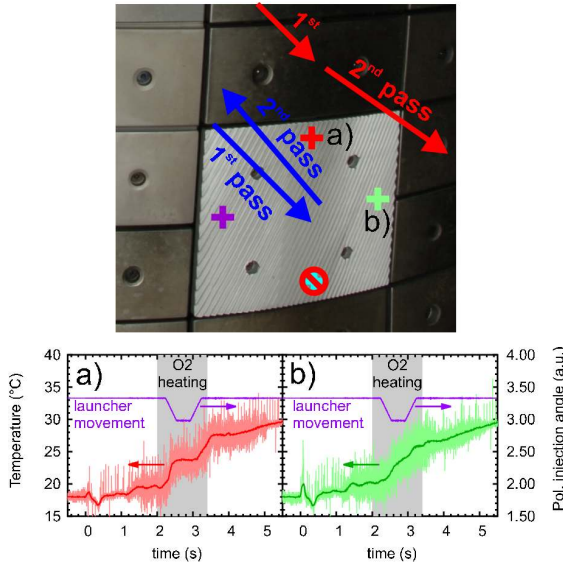

FIG. 5: Thermocouple test scenario. The O2-mode beam was moved from above the holographic mirror to the center of the mirror and back. The time traces of temperatures of the thermocouples are shown in the bottom picture, the red curve (a) and the green (b) curve belongs to the thermocouples in the same colour, the violet line shows the mirror movement and the grey region the O2-mode injection.
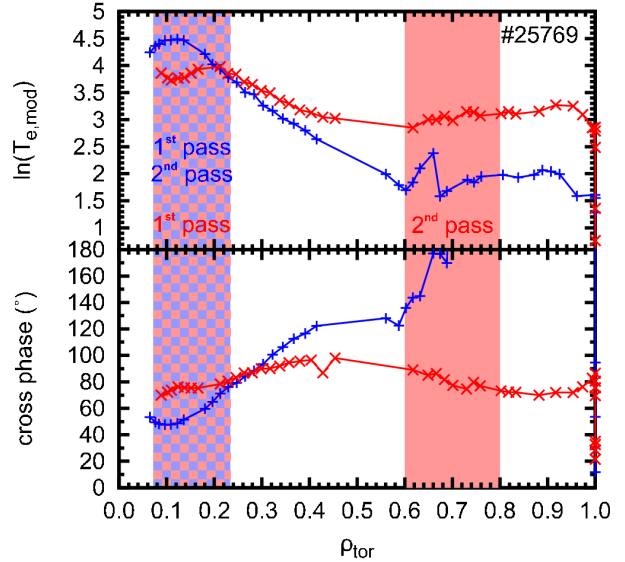
FIG. 6: Fourier analysis of the modulated electron temperature. The O2-mode ECRH was on/off modulated with 30 Hz, the blue curve shows the benefit of the second pass through the plasma center in contrast to the reflection on a standard tile (red curve) above the holographic mirror (see also Fig. 5). The vertical bars indicate the absorption regions for the first and second passes.

In the same discharge it was possible to show the effect of the reflector on the second pass of the O2-mode beam. During the O2-mode heating phase the power of the gyrotron was modulated with 30 Hz. With a movement of the beam from a standard tile above the mirror to the center of the mirror it was possible to compare directly the response of the electron temperature to a second pass.

A Fourier analysis of the electron temperature modulation is depicted in Fig. 6; the blue curve shows the modulation with two passes (beam reflected on mirror) and the red curve with only one pass though the plasma core (beam reflected on a standard tile). It can be seen, that the modulation amplitude in case of the dual pass is higher than for the single pass. The phase also shows a higher absorption in the plasma core in comparison to the single pass. At the edge, the amplitude of the single pass heated plasma is higher and the phase is lower than during the dual pass heating. This is a hint that off-axis heating results from the reflection from the standard tile above the holographic mirror.

4.3 Suppression of tungsten accumulation with O2 heating

The tests in the previous section used plasmas with densities below the X2 cutoff and at least partially X2 heating, such that the tungsten accumulation was no issue. The new ECRH system was not available for most of the 2009 campaign such that only preliminary experiments at the end of the campaign were possible. Fig. 7 shows the first application of O2 heating in a high-triangularity, high-density discharge. Such discharges have to be run with nitrogen seeding to protect from overheating of the divertor [13] and tends to accumulate tungsten. In the first phase, the discharge is heated in X2 mode which is switched off at 2.1 s. O2 heating is switched on at 2.0 s. About 0.2 – 0.3 s later the central tungsten concentration starts to rise indicating that central heating is insufficient, similar to the discharge in Fig. 4 (left). Still we note that when changing from X2 to O2 heating the central temperature does not drop. Also the central density exceeds the X2-cutoff density without a significant rise of the sniffer-probe signal. The latter occurs only as the central temperature drops due to tungsten accumulation such that the single pass absorption is reduced significantly. We note here that also the nitrogen-feedback was not optimal in this discharge. A strong N_2 puff was applied just between 2.1 and 2.3 s and this might have triggered the accumulation process. With more ECRH power, as foreseen for the next campaign, it should be possible to control the tungsten accumulation successfully also above the X2 cutoff.
Central O2 heating was also successfully used in high P/R discharges with 20 MW total heating power [13,14].
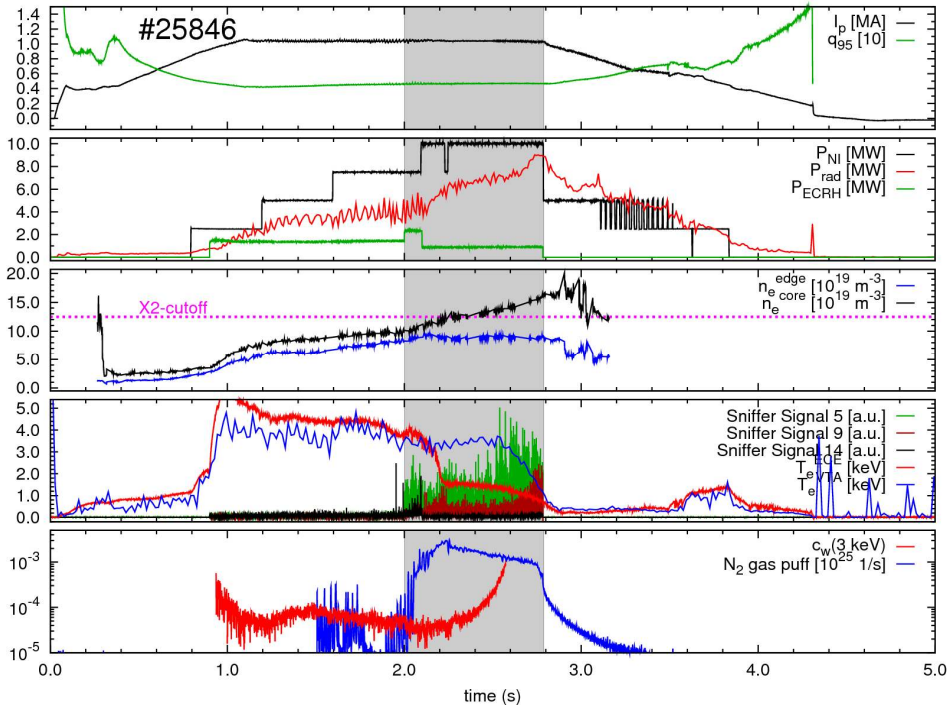

FIG. 7: O2-mode heating of a high-triangularity (δ_o=0.317; δ_u=0.485) plasma at a density over the X2-mode cutoff. The grey region shows the time range where the O2-mode instead of X2-mode is injected. It can be seen, that 1 MW is not sufficient to suppress tungsten accumulation.

5. Conclusion

In this paper new ECR heating scenarios at ASDEX Upgrade where presented. With the O2- and the X3-mode heating, plasma parameters closer to the ITER target values can be achieved in ASDEX Upgrade. However, both modes suffer from incomplete absorption. In the X3-mode heating scenario, the shine-through beam can be absorbed at the X2 resonance at the high field side.

In the O2-mode heating scenario holographic mirrors provide a well defined second pass of the beam and ensure a high absorption (up to 94%). The benefit of the second pass through the plasma was demonstrated in modulation measurements. A first high-performance discharge with O2-mode heating shows promising results. However, 2 MW of ECRH power seem to be necessary for a robust suppression of tungsten accumulation in the regimes studied so far. This power is expected to be routinely available in the next experimental campaign.

References

[1]   NEU, R., et al., Final Steps to an all Tungsten Divertor Tokamak, J. Nucl. Mat. **363-365** (2007) 52–59.

[2]   DUX, R., et al., Influence of the heating profile on impurity transport in ASDEX Upgrade, Plasma Phys. Control. Fusion **45** (2003) 1815.

[3]   WAGNER, D.H., et al., Progress and first Results with the new multifrequency ECRH System for ASDEX Upgrade, IEEE Transactions on Plasma Science **37** (2009) 395–402.

[4]   GANDINI, F., et al., The Detection of the non-absorbed Millimeterwave Power during EC Heating and Current Drive, Fusion Eng. Des. **56-57** (2001) 975–979.

[5]   ERCKMANN, V., GASPARINO, U., Electron Cyclotron Resonance Heating and Current Drive in toroidal Fusion Plasmas, Plasma Phys. Control. Fusion **36** (1994) 1869–1962.

[6]   BORNATICI, M., Theory of Electron Cyclotron Absorption of magnetized Plasmas, Plasma Phys. **24** (1982) 629.

[7]   POLI, E., et al., TORBEAM, a Beam Tracing Code for Electron-Cyclotron Waves in Tokamak Plasmas, Computer Physics Communications **136** (2001) 90–104.

[8]   HÖHNLE, H., et al., Investigation of the O2- and X3-Mode Heating in ASDEX Upgrade. In 36th EPS Conference on Plasma Phys. (2009).

[9]   HÖHNLE, H., et al., O2- and X3-Heating Experiments on ASDEX Upgrade. In Proceedings of 16th Joint Workshop on Electron Cyclotron Emission and Electron Cyclotron Resonance Heating (2010).

[10] MANGOLD, O., et al., Optimization of Microwave Reflection Gratings for Electron Cyclotron Resonance Heating in O2-Mode, In Conference Digest of the 2004 Joint 29th International Conference on Infrared and Millimeter Waves and 12th International Conference on Terahertz Electronics (2004) 717–718.

[11] LEUTERER, F., et al., Status of the new ECRH System for ASDEX Upgrade. Fusion Eng. Des. **74** (2005) 199–203.

[12] STORN, R., On the Usage of differential Evolution for Function Optimization. In Biennial Conference of the North American Fuzzy Information Processing Society (1996) 519–523.

[13] KALLENBACH, A., et al., this conference, IAEA-CN-180/OV/3-1

[14] NEU, R., et al., this conference, IAEA-CN-180/P2-23